A simple nonlinear model of low frequency (interseasonal) oscillations in the tropical atmosphere

D. Luo

Nonlinear Processes in Geophysics (1996) 3: 29 - 40

Nonlinear Processes in Geophysics

A simple nonlinear model of low frequency (intraseasonal) oscillations in the tropical atmosphere

D. Luo

Chengdu Institute of Meteorology, Chengdu, 610041, P.R. China

Received 24 May 1994 - Accepted 16 August 1995 - Communicated by A. Provenzale

Abstract

In this paper, for a prescribed normalized vertical convective heating profile, nonlinear Kelvin wave equations with wave-CISK heating over equatorial region is reduced to a sixth-order nonlinear ordinary differential equation by using the Galerkin spectral method in the case of considering nonlinear interaction between first and second baroclinic modes. Some numerical calculations are made with the fourth-order Rung-Kutta scheme. It is found that in a narrow range of the heating intensity parameter b, 30–60-day oscillation can occur through linear coupling between first and second baroclinic Kelvin wave-CISK modes for zonal wave-number one when the convective heating is confined to the lower and middle troposphere. While for zonal wavenumber two, 30–60-day oscillation can be observed in a narrow range of b only when the convective heating is confined to the lower troposphere. However, in a wider range of this heating intensity parameter, 30–60-day oscillation can occur through nonlinear interaction between the first and second baroclinic Kelvin wave-CISK modes with zonal wavenumber one for three vertical convective heating profiles having a maximum in the upper, middle and lower tropospheres, and the total streamfield of the nonlinear first and second baroclinic Kelvin wave-CISK modes possesses a phase reversal between the upper- and lower-tropospheric wind fields. While for zonal wavenumber two, no 30–60-day oscillations can be found. Therefore, it appears that nonlinear interaction between vertical Kelvin wave-CISK modes favors the occurence of 30–60-day oscillations, particularly, the importance of the vertical distribution of convective heating is reemphasized.

1. Introduction

Since 40–50 day oscillation in the zonal wind in the tropical Pacific was first detected by Madden and Julian (1971, 1972), a series of works on low frequency (intraseasonal) oscillation have been made by many investigators (Yasunari, 1979; Krishnumariti et al., 1982; Murakami et al., 1985; Lau et al., 1985, 1987; Ghil et al., 1990). They found that 30–50 day oscillations in the tropics are dominated by zonal wavenumbers one and two, especially by zonal wavenumber one, and propagate slowly eastward with the phase speed of about 10 m/s, whose vertical structure possesses "baroclinic" feature having the reversal between the upper and the lower levels of troposphere in the wind and pressure fields.

Chang (1974) at first attempted to explain the slow propagation of intraseasonal oscillations using the damping Kelvin waves in tropics. He showed that when cumulus heating and dissipation effects are taken into account, a slowly propagating Kelvin wave mode arises due to a balance between heating and dissipation. Goswami and Shukla (1984) found that interactions between convection and a zonally symmetric circulation can induce intraseasonal oscillations. The numerical study of Lau and Peng (1987) showed that intraseasonal oscillation with period of 30 to 60 days is an intrinsic mode of tropical oscillations maintained by the so-called mobile wave-CISK mechanism due to convective heating. At the same time, Takahashi (1987) pointed out that the vertical distribution of convective heating is very important to control the slow phase speed of intraseasonal oscillation, and further pointed out that a propagating unstable low frequency disturbance can occur only when the interactions between the vertical modes take place. Chang and Lim (1988) investigated in detail the interactions between vertical modes of Kelvin wave-CISK, and suggested that for convective heating with a maximum near the midtroposphere, the CISK modes can propagate eastward at a phase speed between 15 and 30 m/s, which arise from the interaction between two internal modes. And they pointed out that within the framework of linear CISK theory,

their results could not explain the persistence of the "wavenumber-1" structure of the simulated disturbance. The reason is that linear Kelvin wave-CISK mode suffers from "short wave explosion" with its growth rate increasing with the wavenumber. This shows that the linear CISK theory has failed in describing the scale-selection characteristics. Afterwards, in order to overcome this shortcoming, Lim et al. (1990) studied nonlinear wave-CISK modes induced only by nonlinear "positive-only" heating under the condition of neglecting all advective nonlinearity terms. They found that nonlinear "positive-only" heating alone is able to produce exponentially growing "wavenumber-1" flow patterns that propagate with change of shape. However, in all the studies nonlinear advective effect is excluded. If the advective nonlinearity and the wave-CISK heating used by Takahashi (1987) are considered, can this shortcoming be overcome? Recently, Sui and Lau (1989) emphasized that convective heating in the lower troposphere is important in slowing down the Kelvin wave-CISK modes, and also showed that nonlinear effect may play an important role in determining the detailed structure in phase speed and propagation of intraseasonal oscillation in the tropics, to which no theoretical investigation including nonlinear advective effect was presented. Thus, their study leads to increase our belief that under the condition of considering the advective nonlinearity, nonlinear Kelvin wave-CISK mode induced only by the wave-CISK heating may take on a wavenumber-1 structure. Consequently, it is very useful to investigate the combined role of convective heating and advective nonlinearity in producing tropical 30–60 day oscillation.

This paper mainly uses the Galerkin truncated spectral method to examine the role of Kelvin wave-CISK and advective nonlinearity in producing intraseasonal oscillation, particularly, the importance of the vertical distribution of the convective heating is reemphasized. In this paper, in order to simplify our problem, and to emphasize the combined role of both convective heating and advective nonlinearity, two modes of Kelvin wave-CISK are only considered in the vertical direction, and the dissipation is also excluded. In section 2, we introduce basic equations, several normalized convective heating profiles and the obtained spectral truncation equations. Linear and nonlinear results of Kelvin-wave CISK modes for different convective heating profile are given in sections 3 and 4, respectively. In section 5, we give the vertical structures of linear kelvin wave without wave-CISK heating and nonlinear Kelvin wave-CISK mode. Section 6 is devoted to discussions and conclusions.

2. Basic equations, normalized convective heating profiles and truncated spectral equations

2.1 The basic equations

The nonlinear equations describing Kelvin waves with wave-CISK convective heating in the equatorial region can be written

$$(\frac{\partial}{\partial t} + u\frac{\partial}{\partial x} + w\frac{\partial}{\partial z})\frac{\partial u}{\partial z} = -\frac{\partial \theta}{\partial z} \tag{1}$$

$$(\frac{\partial}{\partial t} + u\frac{\partial}{\partial x} + w\frac{\partial}{\partial z})\theta + N^2 w = N^2 b\eta(z)\, w|z = z_0 \tag{2}$$

$$\frac{\partial u}{\partial x} + \frac{\partial w}{\partial z} = 0 \tag{3}$$

where u and w are horizontal and vertical components of wind velocities, respectively;

$\theta = g\frac{\theta'}{\theta_0} = \frac{\partial \phi}{\partial z}$, θ' the disturbance potential temperature, θ_0 the mean potential temperature and g the acceleration speed due to gravity; $\eta(z)$ is the normalized convective heating profile; b is a nondimensional parameter and denotes the intensity of convective heating; N^2 is the Brunt-Vaisala frequency; $w|z = z_0$ is the vertical velocity at the top of boundary layer (z_0 is the height of boundary layer top). Here, the adopted parameterization of convective heating is the so-called wave-CISK scheme proposed by Emanuel (1982), and then applied by Takahashi (1987). When the nonlinear terms in Eqs. (1) and (2) are neglected, this equation is similar in form to that used by Takahashi (1987).

From the continuity equation (1), we may introduce the streamfunction ψ such that it satisfies $u = -\frac{\partial \psi}{\partial z}$ and $w = \frac{\partial \psi}{\partial x}$. In this case, Eqs. (1)–(3) yields

$$\frac{\partial}{\partial t}\frac{\partial^2 \psi}{\partial z^2} + J(\psi, \frac{\partial^2 \psi}{\partial z^2}) = \frac{\partial \theta}{\partial x} \tag{4}$$

$$\frac{\partial \theta}{\partial t} + J(\psi, \theta) + N^2\frac{\partial \psi}{\partial x} =$$

$$N^2 b\eta(z)\frac{\partial \psi}{\partial x}|z = z_0 \tag{5}$$

where ψ and θ vanish at the vertical boundaries $z = 0$ and H,

$J(a,b) = \frac{\partial a}{\partial x}\frac{\partial b}{\partial z} - \frac{\partial a}{\partial z}\frac{\partial b}{\partial x}$ is the Jacobian operator.

For simplicity, we introduce the nondimensional quantities as follows

$$(x,z) = (Lx^*, Hz^*), \psi = LU\psi^* \tag{6}$$

$$\theta = \bar{\theta}\theta^*, t = \frac{L}{U}t^* \tag{7}$$

where the asteriks denote nondimensional forms, L and H are the horizontal and vertical scales respectively, $\bar{\theta} = g\frac{\bar{\theta}_d}{\theta_0}$, $\bar{\theta}_d$ is the characteristic equantity of disturbance potential temperature.

Substituting (6) and (7) into (4) and (5), the nondimensionalization of the two equations and dropping of "*" leads to

$$\frac{\partial}{\partial t}\frac{\partial^2\psi}{\partial z^2} + J(\psi,\theta) = C_A\frac{\partial\theta}{\partial x} \tag{8}$$

$$\frac{\partial\theta}{\partial t} + J(\psi,\theta) + Cd\frac{\partial\psi}{\partial x} =$$

$$C_d b\eta(z)\frac{\partial\psi}{\partial x}|z = z_0 \tag{9}$$

where $C_A = \frac{H\bar{\theta}}{U^2}, C_d = \frac{N^2H}{\bar{\theta}}$ and z_0 is the nondimensional height of boundary layer top.

2.2 The normalized convective heating profile

As a approximate expression of normalized convective heating profile in the tropical atmosphere, we assume $\eta(z) = \lambda_1 \sin(\pi z) + \lambda_2 \sin(2\pi z)$, where $\lambda_1 \leq 1$ and $\lambda_2 \leq 1$. Actually, the prescribed convective heating profile has three special cases: first one is a symmetric heating profile that $\lambda_1 > 0$ and $\lambda_2 = 0$. For this case, if we take $\lambda_1 = 1$ and $\lambda_2 = 0$, the maximum of the convective heating $\eta(z)$ is located in the midtroposphere. This vertical profile is similar to that used by Hayashi (1970) and Takahashi (1987). Second is idealized shallow convective heating profile that $\lambda_1 > 0$ and $\lambda_2 > 0$. For example, if $\lambda_1 = 0.7$ and $\lambda_2 = 0.3$ are allowed, the maximum of the convective heating profile locates in the lower layer of troposphere. This case corresponds to that discussed by Sui and Lau (1989), who found that the convective heating profile having a maximum in the lower troposphere is important for the slower wave-CISK modes. But their results are based on linear theories. Third is idealized deep convective heating profile that $\lambda_1 > 0$ and $\lambda_2 < 0$. For example, if we choose $\lambda_1 = 0.7$ and $\lambda_2 = -0.3$, the maximum of this vertical profile exists in the upper layer of troposphere. Consequently, the convective heating distribution in the tropical atmosphere can be approximately described by the prescribed normalized convective heating profile here.

2.3 The truncated spectral equations

Chang and Lim (1988) have shown that propagating CISK modes can not exist in a linear single vertical mode CISK model. They also found that when convective heating is maximum in the midtroposphere, eastward propagating CISK modes resembling the observed 30–60 day oscillations can occur. These modes result from the interaction between two internal modes which are locked in-phase vertically. Here, in order to study properties of nonlinear Kelvin wave-CISK modes induced only by wave-CISK heating, as a simplest model two modes are considered in the vertical direction. Following the truncated spectral method used by Saltzman (1962) and Lorenz (1963), we seek the solutions of (8) and (9) in the spectral forms

$$\psi = -x_1(t)\sin(kx)\sin(\pi z) - x_2(t)\sin(kx)\sin(2\pi z) \tag{10}$$

$$\theta = x_3(t)\cos(kx)\sin(\pi z) + x_4(t)\cos(kx)\sin(2\pi z) - x_5(t)\sin(2\pi z) - x_6(t)\sin(4\pi z) \tag{11}$$

where $k = \frac{n}{6.371}$ is the nondimensional wavenumber of Kelvin wave-CISK mode, and n is the zonal wavenumber. Here both x_5 and x_6 are considered according to the work of Saltzman (1962). They represent the variations of the vertical potential temperature which are induced through nonlinear interactions between both disturbance streamfield and disturbance potential temperature as seen from the latter discussion.

Substitution of (10) and (11) into (8) and (9), after some algebra, gives

$$\frac{dx_1}{dt} = -\frac{C_A k}{\pi^2}x_3 \tag{12}$$

$$\frac{dx_2}{dt} = -\frac{C_A k}{4\pi^2}x_4 \tag{13}$$

$$\frac{dx_3}{dt} = \pi k x_1 x_5 + kC_d(1 - b\lambda_1 \sin\pi z_0)x_1 - kC_d\lambda_1 b\sin(2\pi z_0)x_2 \tag{14}$$

$$\frac{dx_4}{dt} = 2\pi k x_2 x_6 + kC_d(1 - b\lambda_2 \sin 2\pi z_0)x_2 - kbC_d\lambda_2 \sin(\pi z_0)x_1 \quad (15)$$

$$\frac{dx_5}{dt} = -\frac{k\pi}{2}x_1 x_3 \quad (16)$$

$$\frac{dx_6}{dt} = -k\pi x_2 x_4 \quad (17)$$

In Eqs. (12)–(17), x_1 and x_2 can be called "first and second baroclinic modes", respectively. If Eqs. (12)–(17) is linearized, its analytical solutions can be obtained. However, for nonlinear case the numerical solutions of Eqs. (12)–(17) can be only obtained by means of the fourth-order Rung-Kutta method. Some observations (Murakami et al. 1985) indicated that the tropical intraseasonal oscillation has a "baroclinic" structure with an opposite phase between the upper and lower level of troposphere, which means that the second baroclinic mode x_2 is more important than the first baroclinic mode x_1 in describing the vertical structure of tropical low frequency oscillation. However, because the two modes form the total streamfunction field of tropical intraseasonal oscillation, the first baroclinic mode is also important.

For convenience to compare, we will also give the computational results of the first baroclinic mode. To carry out the numerical calculation, here we may choose the parameters

$U = 10$ m/s, $H = 10^4$ m, $\bar{\theta}_d = \bar{\theta}_0/9.8$ and $z_0 = 0.103$ (the value z_0 is chosen to be the same as that taken by Miyahara (1987)). In this case, we have $C_A = 100$ and $C_d = 1.0$. In addition, the chosen initial amplitudes here are $x_1(0) = x_2(0) = 0.6$ and $x_3(0) = x_4(0) = x_5(0) = x_6(0) = 0.0$, and the time step is chosen to be $\Delta t = 0.173$. In the present paper, to emphasize the role of the advective nonlinearity in producing 30–60 day low frequency oscillations, we will give linear and nonlinear results respectively.

3. Linear Kelvin wave-CISK modes

In this section, we shall study the properties of linear Kelvin wave-CISK modes for various convective heating profile.

If Eqs. (12)–(17) is linearized, they reduce to

$$\frac{dx_1}{dt} = -\frac{kC_A}{\pi^2}x_3 \quad (18)$$

$$\frac{dx_2}{dt} = -\frac{kC_A}{4\pi^2}x_3 \quad (19)$$

$$\frac{dx_3}{dt} = kC_d(1 - b\lambda_1 \sin \pi z_0)\, x_1 - kbC_d\lambda_1 \sin(2\pi z_0)\, x_2 \quad (20)$$

$$\frac{dx_4}{dt} = kC_d(1 - b\lambda_2 \sin 2\pi z_0)\, x_2 - kbC_d\lambda_2 \sin(\pi z_0)\, x_1 \quad (21)$$

For case without wave-CISK, the equations describing x_1 and x_2 are independent from each other, and their periods are different. With T_1 and T_2 denoting the periods of first and second baroclinic modes respectively, then we can obtain $T_1 = 15$ days and $T_2 = 28$ days for case without convective heating. For asymmetric convective heating profile (shallow and deep convective heating profiles) in the vertical direction we can find that both x_1 and x_2 equations are dependent. Clearly, in this case both first and second baroclinic Kelvin wave-CISK modes can interact linearly. As a result, the two modes possesses the same period. Certainly, for symmetric convective heating profile this conclusion may be invalid.

3.1 Zonal wavenumber one

In this subsection, we will devide three cases to discuss our linear results. Here, table 1a–c gives the periods T_1 and T_2 of first and second baroclinic Kelvin wave-CISK modes for different vertical convective heating profiles and different value of b.

Table 1. The periods T_1 and T_2 of linear first and second baroclinic Kelvin wave-CISK modes for zonal wavenumber-one for three vertical convective heating profiles and various b, in which the unit of the period is day: (a) symmetric convective heating profile; (b) shallow convective heating profile; (c) deep convective heating profile.

(a)

b	0	1	2	3	4	5
T_1	15	28	25	60	∞	∞
T_2	28	28	28	28	28	28

(b)

b	0	1	2	3	4	5
T_1	15	33	53	∞	∞	∞
T_2	28	33	53	∞	∞	∞

(c)

b	0	1	2	3	4	5
T_1	15	26	∞	∞	∞	∞
T_2	28	26	∞	∞	∞	∞

3.1.1 Symmetric convective heating profile ($\eta(z) = \sin(\pi z)$)

Table 1a corresponds to the case of symmetric convective heating profile. It is found from this table that

no matter how the intensity of convective heating b is, the second baroclinic mode can only exhibit a nearly 28 day oscillation, while for first baroclinic mode, only when b is between 2.5 and 3.0, its dominant period varies between 30 and 60 days. Actually, the total streamfield of the two modes still oscillates periodically with 28 days over the range of $2.5 \leq b \leq 3.0$ (its figure is omitted). Here, this oscillation can be still called a 30-day oscillation. However, when $b \geq 4.0$ is allowed, this first baroclinic mode will become unstable and stationary. And its growth rate increases with wavenumber. This fact has been noted by Chang and Lim (1988). Certainly, when the convective heating is weaker, the above result is similar to the linear GCM result of Lau et al. (1988), who had shown that the convective heating that has a maximum in the middle layer of troposphere is advantageous to produce about 25-day oscillation for zonal wavenumber-1 which is shorter than that in the observations, and the phase speed of unstable mode can be only lowered to that of the observations (10 m/s, its period is 52 days) by lowering the center of mass of heating.

3.1.2 Shallow convective heating profile ($\eta(z) = 0.7 \sin(\pi z) + 0.3 \sin(2\pi z)$)

Table 1b shows the dependence of the periods of the first and second baroclinic modes on the intensity b of shallow convective heating. We notice that when shallow convective heating profile is considered, both first and second baroclinic modes possess the same period, which will be in the range from 33 to 53 days when b is chosen to be between 1.0 and 2.0. However, as b tends from 3.0 to larger value, the two Kelvin wave-CISK modes will become unstable and stationary.

3.1.3 Deep convective heating profile ($\eta(z) = 0.7 \sin(\pi z) - 0.3 \sin(2\pi z)$)

Table 1c corresponds to the case of deep convective heating profile. It is seen from this table that for deep convective heating profile a propagating Kelvin wave-CISK mode with period of nearly 26 days can be excited through the coupling between the first and second baroclinic modes when $b = 1.0$. However, when $b \geq 2.0$, the two modes become unstable and stationary.

3.2 Zonal wavenumber two

For this zonal wavenumber, our numerical calculations further indicate that for symmetric convective heating profile, the period of the first baroclinic mode is in the range from 30 to 60 days when $2.7 \leq b \leq 3.1$, while when $b \geq 3.2$ this mode will grow. However, for second baroclinic mode its period is nearly 15 days for any value of b. For shallow convective heating profile, when $2.1 \leq b \leq 2.4$, the identical period of both first and second baroclinic modes varies from 30 to 60 days. While when $b \geq 2.5$, the two modes will be unstable and stationary. By comparing with zonal wavenumber one, we can find that when b is only in a narrow range, 30–60-day oscillation can be found for wavenumber two Kelvin wave-CISK modes, which indicating the wavenumber one Kelvin wave-CISK modes can more easily produce tropical 30–60-day oscillation than wavenumber two. However, for deep convective heating profile, no 30–60-day oscillation can be observed even if b is in a moderately extent.

Recently, Sui and Lau (1989) studied the responses of a linear model to two idealized heating profiles such as shallow and deep convective heating profiles, which can be considered as the upper and lower limits of "realistic" heating profiles. They found that for deep convective heating profile (their experiment E_1), a 26-day mode can be observed to travel around the globe. While for shallow convective heating profile (their experiment E_2), a slower eastward moving disturbance with period of 52 days can be excited. In general, according to wave-CISK theory, the most unstable wavenumber-one Kelvin wave possesses 10–20-, 25–30- and 40–50-day period for convective hating that has a maximum in the upper, middle, and lower tropospheres, respectively (Lau and Peng 1987; Sui and Lau 1989). This shows that our linear model is basically capable of describing the main property of linear slow-moving waves-CISK disturbances in the tropical atmosphere. However, recently, the ocean-surface perpetual January $R30$ model performed by Hayashi and Golder (1993) demonstrated that the periods of the simulated intraseasonal oscillations are not extremely sensitive to the vertical heating distributions. They conjectured that this may be due to nonlinear process. Consequently, it appears to be of importance to investigate the dynamical properties of nonlinear Kelvin wave-CISK modes. In next section, we will give the main results of nonlinear Kelvin wave-CISK modes.

4. Nonlinear Kelvin wave-CISK modes and their interaction

In order to clarify differences between linear and nonlinear results, the numerical results of nonlinear Kelvin wave-CISK modes for zonal wavenumbers one and two will be respectively described in detail in this section for the same vertical convective heating profiles as in section 3.

4.1 Zonal wavenumber one

Similar to section 3, we will still devide three cases to discuss our nonlinear results in this subsection.

Table 2a–c describe the dependence of the periods T_1 and T_2 of nonlinear first and second baroclinic modes on the vertical distributions and intensities of convective heating.

Table 2. The periods T_1 and T_2 of nonlinear first and second baroclinic Kelvin wave-CISK modes for zonal wavenumber-one for the same three vertical convective heating profiles as linear case and various b, in which the unit of the period is day: (a) symmetric convective heating profile; (b) shallow convective heating profile; (c) deep convective heating profile.

(a)

b	0	2	4	6	8	...
T_1	15	39	39	39	39	39
T_2	39	39	39	39	39	39

(b)

b	0	1	2	3	4	5
T_1	15	32	48	39	33	28
T_2	39	32	48	39	33	28

(c)

b	0	1	3	5	7	9
T_1	15	32	41	37	32	29
T_2	39	32	41	37	32	29

4.1.1 Symmetric convective heating profile

Table 2a corresponds to the case of symmetric convective heating profile. Obviously, for case without wave-CISK, nonlinear second baroclinic modes can exhibit a 39-day oscillation, while nonlinear first baroclinic mode only has a 15-day period. This property is apparently different from linear wave-CISK theory used above. Therefore, even wave-CISK is excluded, a 39-day oscillation can be also found for second baroclinic mode through nonlinear interaction with first baroclinic mode, whose period is longer than linear case. And its total streamfield also exhibits a 39-day oscillation (its figure is omitted). This conclusion had been recently confirmed by the ocean-surface perpetual January $R30$ model performed by Hayashi and Golder (1993), who showed that both the 40–50- and 25–30-day oscillations can be qualitatively well simulated in a realistic general circulation model, even in the absence of air-sea interactions and cloud-radiation feedback. However, it is interesting to note that when a symmetric convective heating profile that has a maximum in the midtroposphere is considered, both nonlinear first and second baroclinic modes possess the same period through the coupling themselves, and their period is found to be independent of the parameter b. For example, when $b \geq 1.0$, this period is still 39 days, which belongs to the 30–60 day period range.

Figures 1a and 1b give the evolution solutions of x_1 and x_2, and the phase trajectories (x_2, x_4), (x_1, x_3), (x_2, x_3) and (x_1, x_4) of nonlinear system (12)–(17) for = 2.0 and 4.0, respectively. It is found that for both b = 2.0 and 4.0 the time-evolutions of x_2 are the same, and their phase trajectories (x_2, x_4) are also the same. But the other phase trajectories vary slightly with the change of b. In addition, we note that the time-evolution of x_1 appears to exhibit chaotic behavior, which can be seen from the calculation of Lyapunov exponent hereafter.

4.1.2 Shallow convective heating profile

Table 2b describes the dependence of the periods of nonlinear first and second baroclinic modes on the intensity parameter b of shallow convective heating profile, where T_1 and T_2 are assigned to be the dominant periods of nonlinear first and second baroclinic modes, respectively. From this table we can find that when a shallow convective heating profile is considered as wave-CISK heating both nonlinear first and second baroclinic modes still have the same period. When b varies from 1.0 to 5.0, this period will decrease from 55 to 28 days. Comparing this result with linear case in table 1b, we notice that under the same conditions the parameter domain of b for a 30–60-day oscillation to occur in nonlinear theory is wider than that in linear theory. This shows that the advective nonlinearity favors the appearance of 30–60-day oscillation. Certainly, if $b > 5.0$ is allowed, the periods of the two modes will belong to the 25–30-day period band.

Figure 2 shows the dependence of the evolution solutions of x_1 and x_2, and the phase trajectories (x_2, x_4), (x_1, x_3), (x_2, x_3) and (x_1, x_4) of nonlinear system (12)–(17) on the intensity parameter b of shallow convective heating profile. Figure 2a corresponds to the case of b = 1.0. Notice that when b = 1.0 x_2 oscillates periodically with 55 days, while x_1 oscillates quasi-periodically with the same dominant period. In this case, the phase trajectories of system (12)–(17) are seen to be the limit cycles. Figure 2b describes the case of b = 3.0. It is found that for this case the solutions of x_1 and x_2 are chaotic, which can be found from the phase trajectories given in figure 2b. Moreover, both x_1 and x_2 are found to oscillate with a doubled period, and their dominant period is near 39 days. Here, if when b continues to increase, the chaotic behavior of both x_1 and x_2 seems to be more clear. For example, in figure 2c for b = 5.0 this point can be clearly found. On the other hand, in order to examine the chaotic behavior of the solutions of Eqs. (12)–(17), according to Lin (1993) we compute the Lyapunov exponents of system (12)–(17), and the obtained Lyapunov exponents are LE_1 = 0.0152, LE_2 = – 0.0026, LE_3 = 0.0128, LE_4 = 0.0119, LE_5 = 0.00292 and LE_6 = – 0.0166. These Lyapunov exponents indicate that for b = 5.0, the solutions of Eq.

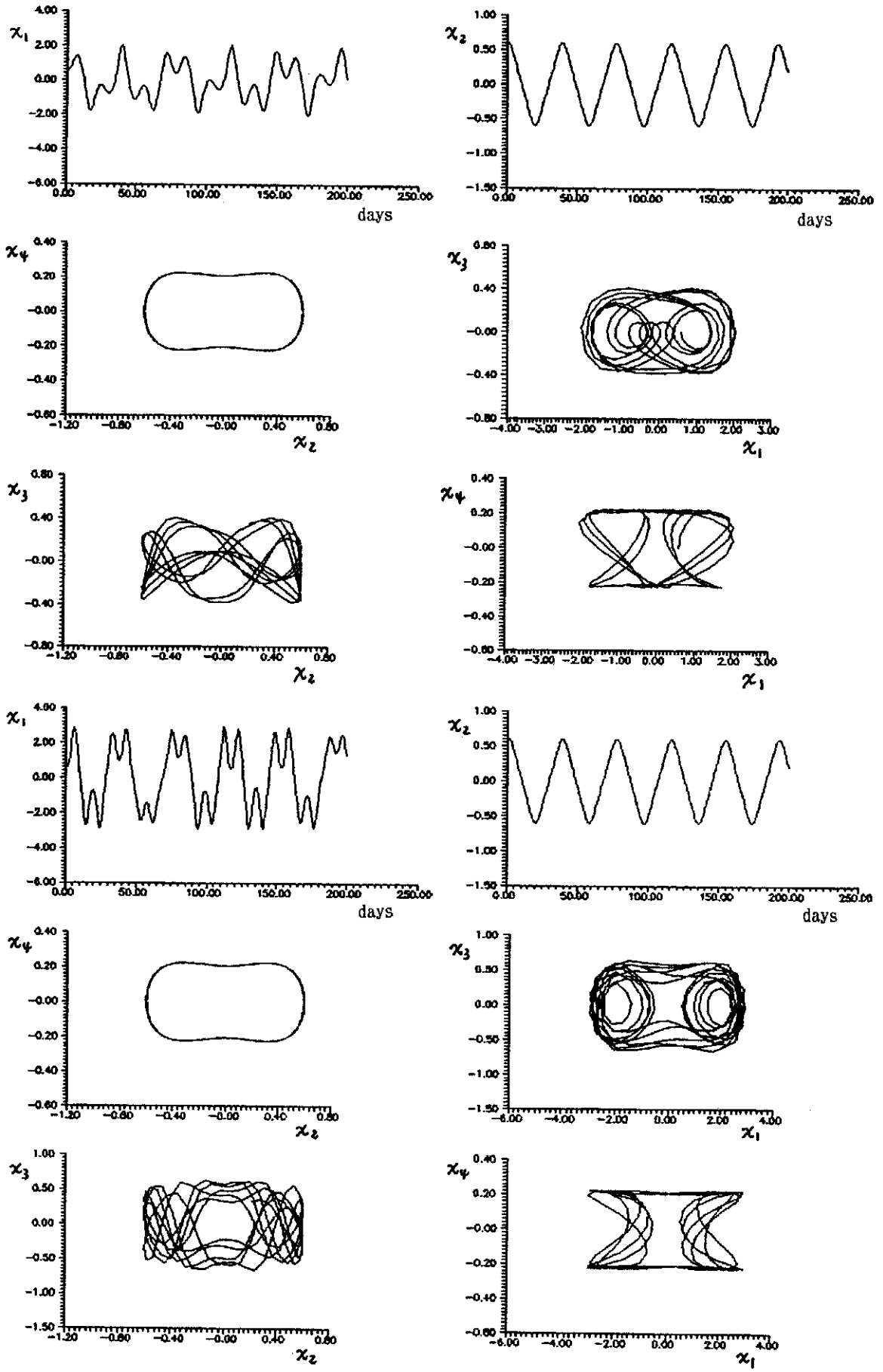

Fig. 1. The evolution solutions of x_1 and x_2, and the phase trajectories (x_2, x_4), (x_1, x_3), (x_2, x_3) and (x_1, x_4) for nonlinear system (12)–(17) for symmetric convective heating with $b = 2.0$ and 4.0, respectively: (a) $b = 2.0$; (b) $b = 4.0$.

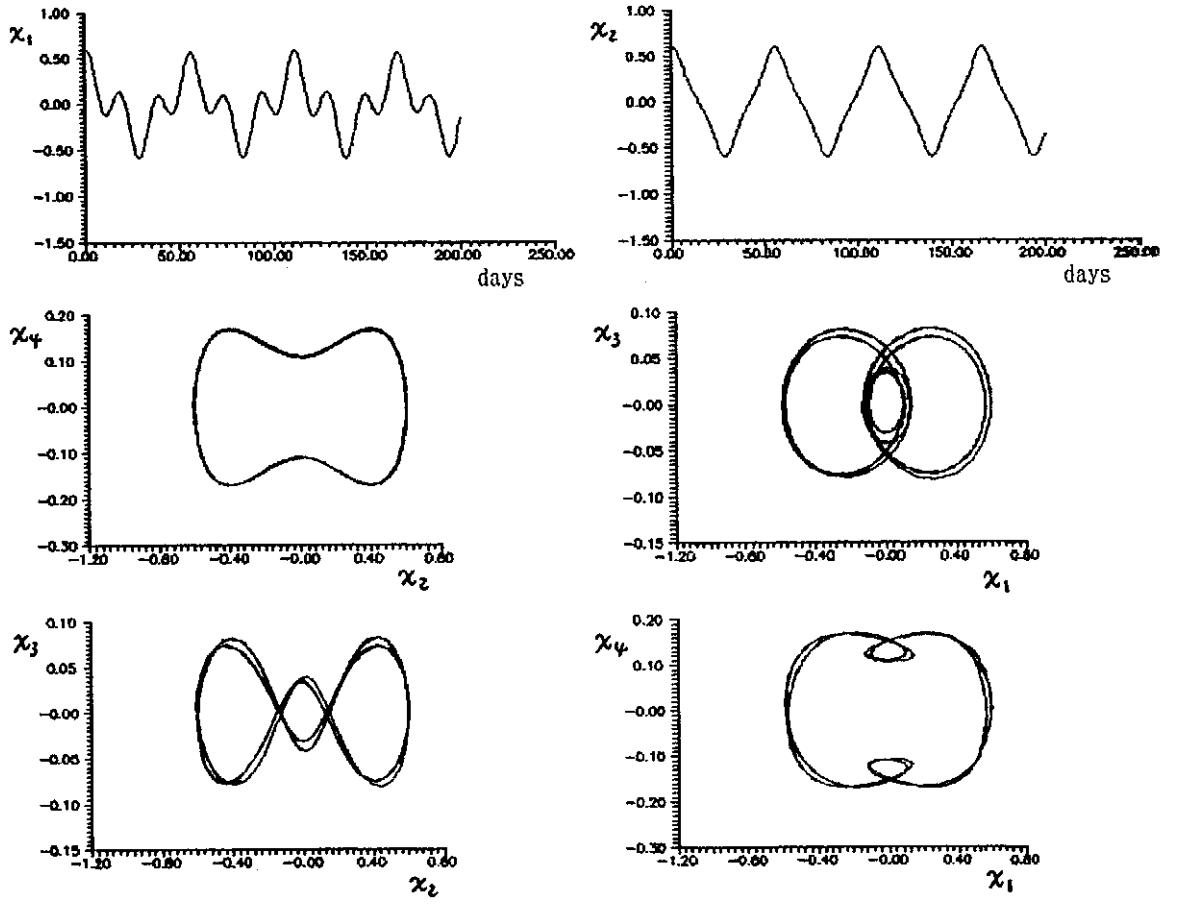

(a)

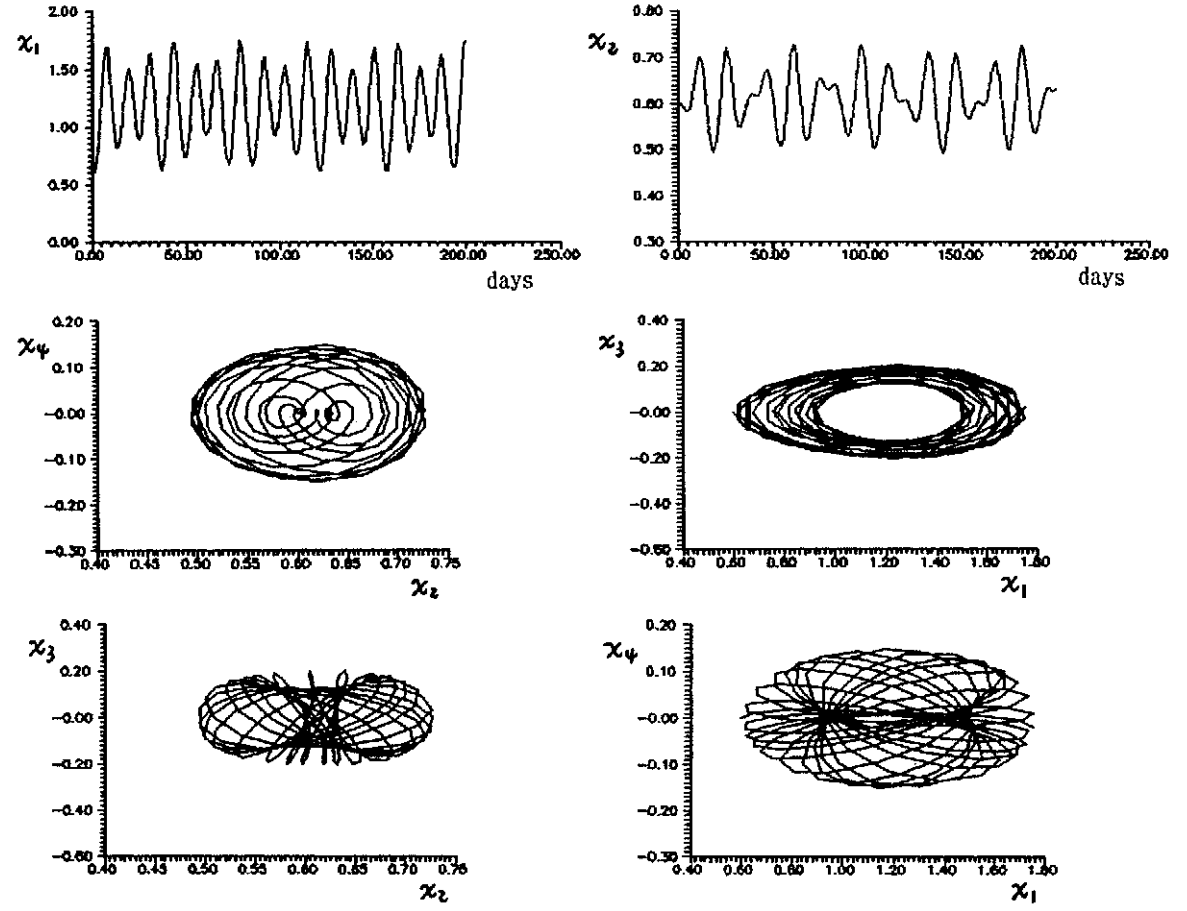

(b)

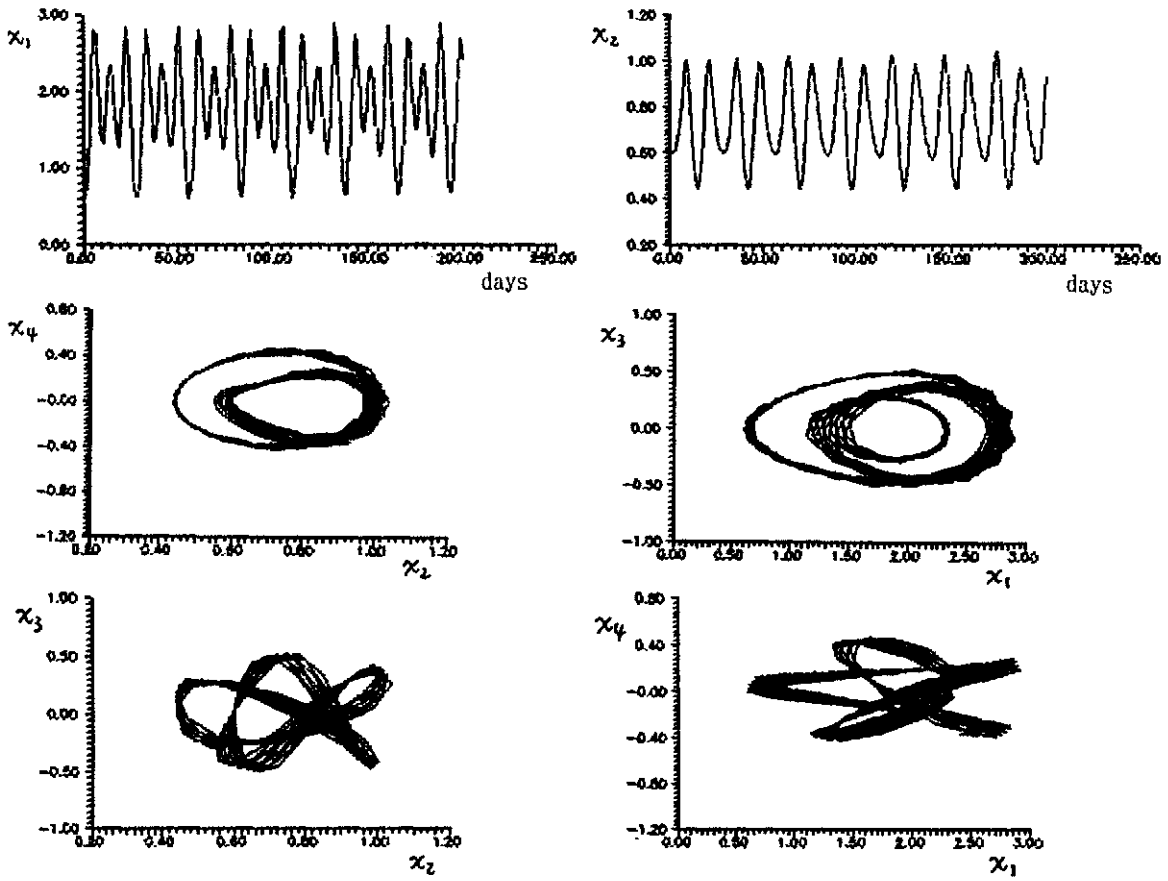

Fig. 2. The evolution solutions of x_1 and x_2, and the phase trajectories (x_2, x_4), (x_1, x_3), (x_2, x_3) and (x_1, x_4) of nonlinear system (12)–(17) for shallow convective heating profile with $b = 1.0$, 3.0 and 5.0, respectively: (a) $b = 1.0$; (b) $b = 3.0$; (c) $b = 5.0$.

(6) are chaotic. For a fixed b the nonperiodicity can be observed, but its dominant period is dependent on the intensity parameter b.

4.1.3 Deep convective heating profile

Table 2c corresponds to the case of deep convective heating profile. It is found that when b is between 1.0 and 9.0, a low frequency oscillation in the 29–41-day period band can occur through nonlinear coupling between first and second baroclinic modes. This shows that although a deep convective heating profile same as linear model is considered, 30–60 day oscillation can be still observed in a wide range of the parameter b. This conclusion is remarkably different from the result of linear Kelvin wave-CISK modes with deep convective heating. In addition, the evolution solutions of x_1 and x_2, and the phase trajectories of system (12)–(17) for this case are omitted here.

4.2 Zonal wavenumber two

For three vertical heating distributions prescribed here, no 30–60-day oscillation can be found for zonal wavenumber two Kelvin wave-CISK modes. When b is moderate, quasi-20-day oscillations can be only detected for the three cases, and their figures have been omitted here. Therefore, there is a great difference between linear and nonlinear results for zonal wavenumber two Kelvin wave-CISK modes.

The numerical calculations in this section demonstrate that in a wide range of the parameter b, 30–60-day oscillation can occur through nonlinear coupling between both first and second baroclinic modes with zonal wavenumber-one for three different heating profiles, and the period of nonlinear low frequency oscillation obtained here is found to be not extremely sensitive to the vertical distribution of convective heating, but the period length of this oscillation still depends on the vertical distribution of convective heating for the same parameter b. This conclusion is basically consistent with the property of the simulated oscillation obtained by Hayashi and Golder (1993), who showed that the simulated low frequency oscillation is not extremely sensitive to the vertical distribution of convective heating. While for linear coupling between the two modes, 30–60-day oscillations can be only detected in a narrower range of the parameter b, but the vertical heating profile must be required to have a maximum in the lower or the middle level of troposphere. Recently, Zhao and Ghil (1991) have shown that nonlinear symmetric instab-

ility could explain 25–30-day oscillation, but it fails to explain 40–50-day oscillation. However, our nonlinear theory presented here seems to be able to explain the 40–50-day peak of the simulated oscillations obtained by Hayashi and Golder (1993).

5. The vertical structures of linear free Kelvin wave and nonlinear Kelvin wave-CISK mode for zonal wavenumber one

In this section, in order to emphasize the role of the advective nonlinearity and wave-CISK heating in tropical intraseasonal oscillation, we at first give the vertical streamfield structure of linear wavenumber-one Kelvin wave without wave-CISK heating.

Figure 3 shows the time-sequence of the vertical structure of linear Kelvin wave for zonal wavenumber-one without wave-CISK heating for the initial values $x_1(0) = x_2(0) = 0.6$, and $x_3(0) = x_4(0) = x_5(0) = x_6(0) = 0.0$. It is found that in the case without wave-CISK heating, the "baroclinic" structure with a opposite phase between the upper and lower level of troposphere of the linear Kelvin wave is not clear. Moreover, we notice that the total vertical streamfield of the Kelvin wave oscillates with the 29-day period, which is near the period of the second baroclinic mode. This indicates that the total vertical streamfield of linear Kelvin wave for zonal wavenumber-one without wave-CISK heating is basically unable to describe the vertical structure of tropical intraseasonal oscillations. However, for linear wavenumber-one Kelvin wave-CISK mode with shallow convective heating, its vertical streamfield has a phase reversal between the upper- and lower-tropospheres when b is between 1.0 and 2.0 (its figure has been omitted). Therefore, linear wavenumber-one Kelvin wave-CISK modes with shallow convective heating profile can explain the 30–60-day peak and the vertical structure of intraseasonal oscillations at the equator.

Figure 4 shows the time-sequence of the total vertical streamfield of nonlinear Kelvin wave-CISK mode with zonal wavenumber one for shallow convective heating profile, in which $b = 1.0$ and the same initial conditions as in figure 3 are allowed. It is noted that the initial streamfield of the nonlinear Kelvin wave-CISK mode prescribed here is the same as in figure 3a, as shown in figure 4a. Due to the action of wave-CISK heating, the vertical structure of the nonlinear Kelvin wave-CISK mode at day 28 exhibits a phase reversal between the upper- and lower-tropospheres, which can be seen from figure 4b. And this vertical structure is found to be able to be maintained in its evolution process. It is worth noting that at day 83 the same vertical structure as in figure 4b reappears, which indicating that the cycle period of the vertical structure of nonlinear wavenumber-one Kelvin wave-CISK mode for $b = 1.0$ is close upon 55 days, which is the same as in table 2b for $b = 1.0$. Therefore, the results obtained here show that the vertical streamfield of nonlinear wavenumber-one Kelvin wave-CISK mode can describe the vertical structure of intraseasonal oscillation in the tropical atmosphere when all the parameters are moderate. For the streamfields of the other nonlinear wavenumber-one Kelvin wave-CISK modes, they have been omitted here.

6. Conclusions and discussions

In this paper, we have investigated the dynamical properties of linear and nonlinear Kelvin wave-CISK modes for three vertical heating profiles, respectively. It is found that in a narrow range of the heating intensity parameter b, 30–60-day oscillation can occur through linear interaction between two vertical baroclinic modes for zonal wavenumber-one when the convective heating is confined to the lower and middle tropospheres. While for zonal wavenumber two, 30–60-day oscillation can be observed only when the convective heating is confined to the lower tropospheres, and the range of the required parameter is narrower. This mechanism was first proposed by Chang and Lim (1988). When b is larger, the two baroclinic modes may be unstable and stationary. In this case, its growth rate increases with the wavenumber. However, for nonlinear model, nonlinearity in system (12)–(17) will suppress linear growth and lead to finite-amplitude oscillations. Our numerical results obtained here indicate that for three convective heating profiles that have a maximum in the upper, middle, and lower troposphere respectively, in a wider range of the heating intensity parameter b nonlinear coupling between first and second baroclinic modes with zonal wavenumber-one can produce intraseasonal oscillation in the 30–60-day period band, but for zonal wavenumber two no 30–60-day oscillation can be found. This shows that nonlinear 30–60-day oscillation tends to take on the wavenumber-1 structure. In addition, the streamfield of nonlinear wavenumber-one Kelvin wave-CISK mode extremely resembles the vertical structure of the observed 30–60-day oscillation that has a phase reversal between the upper- and lower-tropospheres, and its wavenumber-1 shape can be maintained. Therefore, it appears that the combination of the advective nonlinearity and wave-CISK heating is advantageous to the appearance of 30–60-day oscillations in the tropical atmosphere.

The above conclusions are aimed at the nondissipative case. The very weak dissipation doesn't greatly affect the periods of Kelvin wave-CISK modes if we consider the dissipation in Eqs. (12)–(17). However, if dissipation is too strong, it will

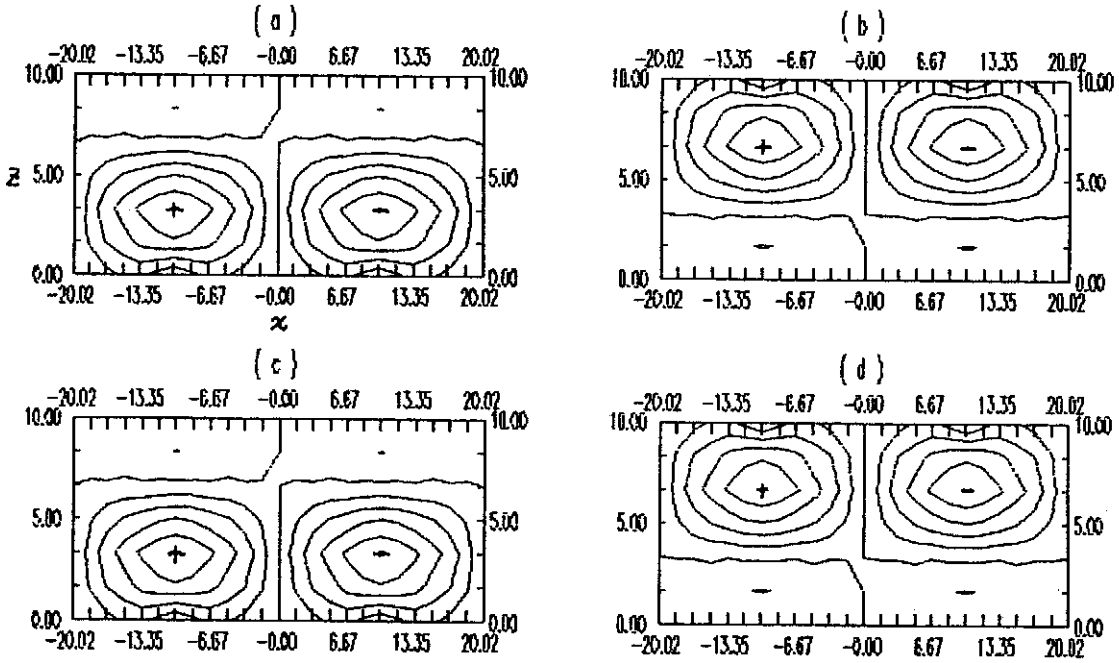

Fig. 3. The time sequences of the total vertical streamfield of linear wavenumber-one Kelvin wave without wave-CISK heating for the initial values $x_1(0) = x_2(0) = 0.6$, $x_3(0) = x_4(0) = x_5(0) = x_6(0) = 0.0$, in which the vertical coordinate has been enlarged 10 times: (a) day 0; (b) day 15; (c) day 29; (d) day 44. The contour interval is 0.2.

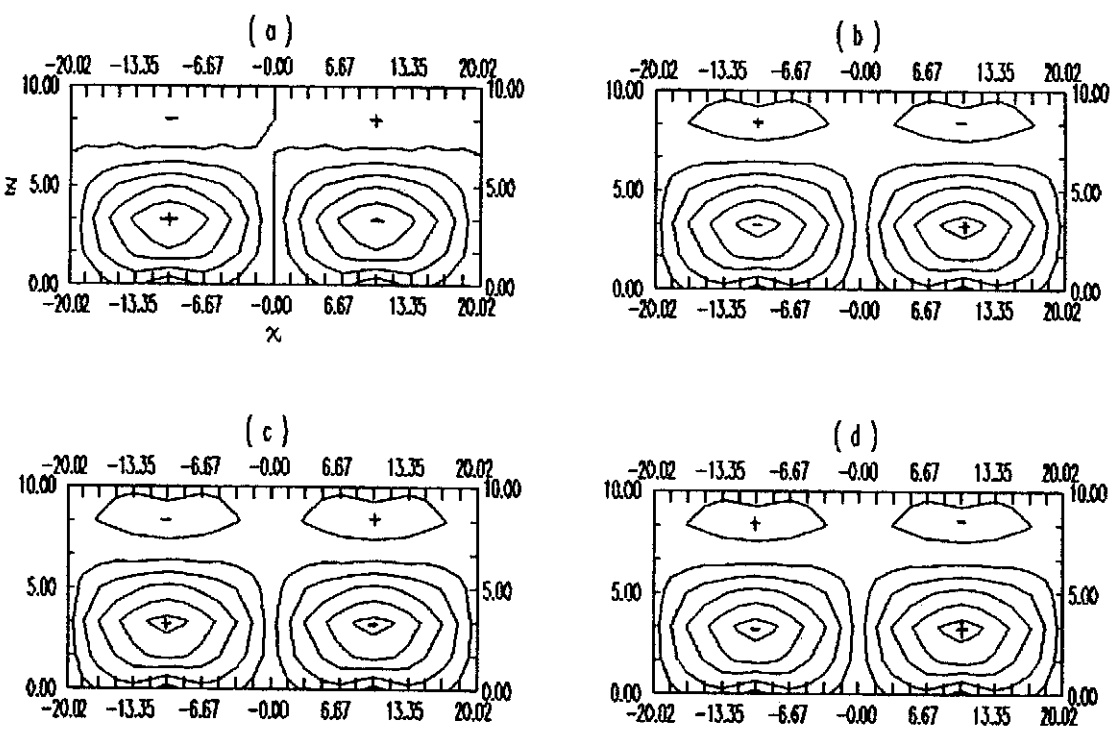

Fig. 4. The time-sequences of the total streamfield of nonlinear wavenumber-one Kelvin wave-CISK mode for shallow convective heating profile with the same initial conditions as in figure 3 and for $b = 1.0$; (a) day 0; (b) day 28; (c) day 56; (d) day 83. The contour interval is 0.2.

make Kelvin wave-CISK modes decay. This problem will not be discussed in detail in this paper.

Acknowledgements. This project has been supported by Sichuan Youth Science and Technology Foundation.

References

Chang, C.P., Viscous internal gravity waves and low frequency oscillations in the tropics, J. Atmos. Sci., 34, 901–910, 1974.

Chang, C.P., and Lim, H., Kelvin wave-CISK: A possible mechanism for the 30–50 day oscillations. J. Atmos. Sci., 45, 1709–1720, 1988.

Emanuel, K.A., Intertial instability and mesoscale convective system. Part II: Symmetric CISK in a baroclinic flow, J. Atmos. Sci., 39, 1080–1097, 1982.

Ghil, M., and Mo, K.C., Intraseasonal oscillation in the global atmosphere. Part I: Northern Hemisphere and tropics, J. Atmos. Sci., 48, 752–790, 1991.

Hayashi, Y., and Golder, D.G., Tropical 40–50 and 25–30-day oscillations appearing in realistic and idealized GFDL climate models and the ECMWF dataset, J. Atmos. Sci., 50, 464–494, 1993.

Knuston, T.R., and Weickmann, K.M., 30–60-day atmospheric oscillations: Composite life cycles of convective heating and circulation anomalies, Mon. Wea. Rev., 115, 1407–1436, 1987.

Krishnamurti, I.N., and Subrahmanyam, D., The 30–60-day mode at 850 mb during MONEX, J. Atmos. Sci., 39, 2088–2095, 1982.

Lau, N.C., T.M. Held and Neelin, J.D., The Madden-Julian oscillation in an idealized general circulation model. J. Atmos. Sci., 45, 3810–3832, 1988.

Lau, K.M., and Chan, P.H., Aspects of the 40–50-day oscillation during the northern winter as inferred from outgoing longwave radiation, Mon. Wea. Rev., 113, 1889–1909, 1985.

Lau, K.M., and Peng L., Origin of low frequency (intraseasonal) oscillations in the tropical atmosphere. Part I: Basic theory, J. Atmos. Sci., 44, 2023–2047, 1987.

Lim, H., Lim, T.K., and Chang, C.P., Reexamination of wave-CISK theory: Existence and properties of nonlinear wave-CISK modes, J. Atmos. Sci, 47, 3078–3091, 1990.

Lin, Z.S., Nonlinear dynamics and atmospheric sciences, Nanjing University Press, 350, 1993.

Lorenz, E.N., Deterministic nonperiodic flow, J. Atmos. Sci., 20, 130–140, 1963.

Madden, R.A., and Julian, P.R., Detection of a 40–50 day oscillation in the zonal wind in the tropical Pacific, J. Atmos. Sci., 28, 702–708, 1972.

Madden, R.A., and Julian, P.R., Description of global-scale circulation cells in the tropic with a 40–50 day period. J. Atmos. Sci., 29, 1109–1123, 1973.

Miyahara, S., A simple model of the tropical intraseasonal oscillation, J. Meteor. Soc. Japan, 65, 341–351, 1987.

Murakami, T., and Nakazawa, T., Tropical 45 day oscillations during the 1979 Northern Hemisphere, J. Atmos. Sci., 42, 1107–1122, 1985.

Saltzman, B., Finite amplitude free convection as a initial value, J. Atmos. Sci., 19, 329–341, 1962.

Sui, C.H., and Lau, K.M., Origin of low frequency (intraseasonal) oscillations in the tropical atmosphere. Part II: Structure and propagation of mobile wave-CISK modes and their modification by lower boundary forcing, J. Atmos. Sci., 46, 37–56, 1989.

Takahashi, M., A theory of the slow phase speed of intraseasonal oscillation using the wave-CISK, J. Meteor, Soc. Japan, 65, 43–49, 1987.

Yamagata, T., A simple moist model relevant to the origin of intraseasonal disturbance in the tropics, J. Meteor. Soc. Japan 65, 153–165, 1987.

Yasunari, T., Cloudiness fluctuations associated with the Northern Hemisphere summer monsoon, J. Meteor. Soc. Japan, 57, 227–242, 1979.

Zhao, J.X., and Ghil, M., Nonlinear symmetric instability and intraseasonal oscillations in the tropical atmosphere, J. Atmos. Sci., 48, 2552–2568, 1991.